

Review

# Recent Progress on Ruthenium-Based Electrocatalysts towards the Hydrogen Evolution Reaction

Lulu Li, Fenyang Tian, Longyu Qiu, Fengyu Wu , Weiwei Yang \* and Yongsheng Yu \*

State Key Laboratory of Urban Water Resource and Environment, School of Chemistry and Chemical Engineering, Harbin Institute of Technology, Harbin 150001, China; lululu.081@gmail.com (L.L.); tianfenyang1995@gmail.com (F.T.); qiulongyu1997@gmail.com (L.Q.); 23b925070@stu.hit.edu.cn (F.W.)

\* Correspondence: yangww@hit.edu.cn (W.Y.); ysyu@hit.edu.cn (Y.Y.)

**Abstract:** Hydrogen has emerged as an important candidate for clean energy, owing to its environmentally friendly advantages. Electrolytic hydrogen production stands out as the most promising technology for hydrogen production. Therefore, the design of highly efficient electrocatalysts is significant to drive the application of hydrogen technologies. Platinum (Pt)-based catalysts are famous for their outstanding performance in the hydrogen evolution reaction (HER). However, the expensive cost limits its wide application. Ruthenium (Ru)-based catalysts have received extensive attention due to their relatively lower cost and HER performance similar to that of Pt. Nevertheless, the performance of Ru-based catalysts is still unable to meet industrial demands. Therefore, improving HER performance through the modification of Ru-based catalysts remains significant. In this review, the reaction mechanism of HER is analyzed and the latest research progress in the modification of Ru-based electrocatalysts is summarized. From the reaction mechanism perspective, addressing the adsorption of intermediates on the Ru-based electrocatalyst surface, the adsorption–activation of interface water molecules, and the behavior of interface water molecules and proposing solutions to enhance performance of Ru-based electrocatalyst are the main findings, ultimately contributing to promoting their application in the field of electrocatalysis.

**Keywords:** hydrogen evolution reaction; ruthenium; water splitting; electrocatalysts



**Citation:** Li, L.; Tian, F.; Qiu, L.; Wu, F.; Yang, W.; Yu, Y. Recent Progress on Ruthenium-Based Electrocatalysts towards the Hydrogen Evolution Reaction. *Catalysts* **2023**, *13*, 1497. <https://doi.org/10.3390/catal13121497>

Academic Editor: Jae Sung Lee

Received: 30 October 2023

Revised: 30 November 2023

Accepted: 5 December 2023

Published: 7 December 2023



**Copyright:** © 2023 by the authors. Licensee MDPI, Basel, Switzerland. This article is an open access article distributed under the terms and conditions of the Creative Commons Attribution (CC BY) license (<https://creativecommons.org/licenses/by/4.0/>).

## 1. Introduction

Currently, the consumption of fossil fuels has resulted in serious environmental pollution. There is an urgent need to develop clean energy technologies to address this issue. Hydrogen (H<sub>2</sub>), with its high energy density and non-polluting combustion products, has received widespread attention in recent years [1–3]. The primary technologies for large-scale H<sub>2</sub> production at present include methanol decomposition [4–6], ammonia decomposition [7–9], biomass conversion [10–12], photocatalytic water splitting [13] and electrochemical water splitting. Methanol decomposition produces CO<sub>2</sub>, while ammonia decomposition generates N<sub>2</sub>, which requires further purification. Biomass and photocatalytic H<sub>2</sub> production technologies have low efficiency and complex processes, making them less promising compared to electrochemical water splitting for H<sub>2</sub> production. Electrochemical water splitting, using water as the reactant and allowing for the separation of anode and cathode chambers, can achieve hydrogen purity levels as high as 99.9%. However, the development of electrochemical water splitting for H<sub>2</sub> production is constrained by high costs and low-efficiency electrocatalysts [14,15]. Therefore, delving into the mechanism of the hydrogen evolution reaction (HER) and designing low-cost highly effective catalysts are vital research objectives [16].

Researchers have made significant efforts in the search for high-performance catalyst materials. Many materials have been developed in HER, including alloys, sulfides, phosphides, nitrides, and carbides, as well as various composite materials. Pt is considered the

best HER electrocatalyst, but its high cost, low reserves and unsatisfactory stability limit its widespread application [17]. Ru has the lowest price (only 1/4 of Pt) among the platinum group metals (PGM). Meanwhile, it exhibits similar performance with Pt [18]. Therefore, Ru-based catalysts have gained extensive attention as a promising candidate. However, due to the unfilled valence shell electronic structure of Ru, the surface of Ru-based catalysts often exhibits too strong hydrogen adsorption, resulting in sluggish HER kinetics [19–21]. Additionally, the high reduction potential and cohesive energy of Ru have always made it challenging to control the morphology and crystal phases of Ru-based nanomaterials.

This review focuses on the research progresses of Ru-based HER electrocatalysts [22,23]. First, the reaction process and mechanism of HER are briefly summarized [24–26]. Subsequently, the relationship between the adsorption of intermediates and the electronic structure of Ru-based catalysts are analyzed. Additionally, the adsorption and activation process of water molecules on the catalyst surface in neutral and alkaline-pH environments are discussed, along with the corresponding enhancement strategies [27]. Furthermore, due to the significant impact of mass transfer at high currents, the interfacial water behavior and control strategies of Ru-based catalysts are briefly introduced. Finally, the problems in the development of Ru-based HER electrocatalysts and the future directions are proposed [28,29].

This review addresses the research gap by delving into the modification of Ru-based catalysts to enhance their HER performance from the reaction mechanism perspective. The main finding stems from a detailed exploration of the adsorption of intermediates on the Ru-based electrocatalyst surface, the adsorption–activation of interface water molecules, and the behavior of these interface water molecules. The study aims to provide researchers with new insights for the deeper design and modification of Ru-based catalysts by summarizing the research progress of Ru-based catalysts from a mechanism perspective. Ultimately, it will contribute to the development of highly efficient, cost-effective catalysts that can find widespread industrial application in the future.

## 2. Mechanisms of HER

A typical electrolysis cell for hydrogen production consists of a cathode, an anode, an electrolyte, and a power source. Half-reactions for hydrogen evolution (HER) and oxygen evolution occur at the cathode and anode, respectively. The HER at the cathode is described as follows:



HER is a multi-step reaction occurring at the cathode surface (Table 1) [30–32]. In acidic conditions, the HER reaction pathway involves the Volmer–Heyrovsky or Volmer–Tafel reactions. Different from HER in acidic electrolytes, the initial step of alkaline and neutral-pH HER involves the dissociation of adsorbed water into  $\text{H}^*$  and  $\text{OH}^-$ . Notably, the reaction kinetics for HER in alkaline and neutral-pH conditions are significantly slower, at least two orders of magnitude slower than in acidic conditions. The low reaction rate is attributed to three factors: the slower transport rate of  $\text{OH}^-$  ions, the higher energy barrier to break O-H bonds in water molecules than to hydrate protons, and the different adsorption capabilities for hydrogen in acidic or alkaline environments.

**Table 1.** Basic reaction steps of HER in acidic and neutral/alkaline reaction conditions.

Condition	Acidic	Neutral/Alkaline
Total reaction	$2\text{H}^+ + 2\text{e}^- \rightarrow \text{H}_2$	$2\text{H}_2\text{O} + 2\text{e}^- \rightarrow \text{H}_2 + 2\text{OH}^-$
Volmer	$\text{H}^+ + \text{e}^- \rightarrow \text{H}^*$	$\text{H}_2\text{O} + \text{e}^- \rightarrow \text{H}^* + \text{OH}^-$
Tafel	$2\text{H}^* \rightarrow \text{H}_2$	$2\text{H}^* \rightarrow \text{H}_2$
Heyrovsky	$\text{H}^+ + \text{e}^- + \text{H}^* \rightarrow \text{H}_2$	$\text{H}_2\text{O} + \text{e}^- + \text{H}^* \rightarrow \text{H}_2 + \text{OH}^-$

### 3. Intermediate Adsorption on Ru-Based Catalyst Surfaces

Despite the fact that the HER produces only H<sub>2</sub>, it involves multiple reaction steps, including adsorption–activation–desorption processes. In other words, apart from the steps that protons are assembled and formed H<sub>2</sub>, progresses such as the adsorption and activation of H<sub>2</sub>O, H<sub>2</sub>O cleavage, and the transport of byproduct OH<sup>−</sup> significantly affect the electrocatalytic HER. Having a further study of reaction mechanisms is essential for catalyst design to improve the performance of catalyst.

Optimizing the adsorption of intermediate species on the surface of the catalyst is critical for HER. For the Ru-based catalysts, it means optimizing the binding affinity and stability between the reactive intermediates with the Ru surface. The strategies involve changing the composition, structure, or surface properties of catalyst to create more favorable adsorption sites for the intermediates. Tuning the electronic properties of the Ru atoms, introducing suitable ligands or co-catalysts, or modification the morphology of catalyst to expose more active sites can be adopted. Additionally, controlling the surface coverage of intermediates and minimizing competing reactions, such as desorption or over-oxidation, are essential for efficient catalysis.

#### 3.1. Hydrogen Adsorption

According to the Sabatier theory, the adsorption of protons at active sites should neither be too strong nor too weak. Adsorption and desorption should maintain equilibrium to achieve optimal reaction activity. If H adsorption is too strong, the Tafel step would be limited, making it challenging for adsorbed H to assemble into H<sub>2</sub>. Furthermore, the generated H<sub>2</sub> is also trapped due to excessive adsorption, leading to catalyst poisoning. On the other hand, weak adsorption makes it difficult for H to separate from H<sub>2</sub>O or hydrated hydrogen ions. Additionally, when the adsorption is too weak, it directly reduces the probability of effective collisions and the generation of H<sub>2</sub>. The moderate adsorption leads to a high exchange current density, which is the key criterion for catalyst material design and selection.

It is worth noting that, in order to reasonably control the hydrogen adsorption free energy ( $\Delta G_{H^*}$ ) on catalyst surfaces, researchers have embarked on extensive theoretical explorations. The widest theory is the *d*-band center theory proposed by Nørskov. This theory put forward that the *d*-band center plays an important role in predicting the adsorption strength of the interactions. Specifically, when the *d*-band center is located relatively close to the Fermi level, the anti-bonding orbital of the metal-hydrogen (M-H) bonds are less likely to electron filling, resulting in more stable M-H bond and strong adsorption.

#### 3.2. Intermediate Adsorption Modification Strategies

Pt is universally accepted as the best catalyst for HER. The strategy of emulating the electronic structure of Pt to design Ru-based catalysts to produce Pt-like H adsorption–desorption characteristics represents a reliable approach. The outer electron configuration of Pt is [Xe]6s<sup>1</sup>4f<sup>14</sup>5d<sup>9</sup> and that of Ru is [Kr]5s<sup>1</sup>4d<sup>7</sup>. Pt has two unpaired electrons in its outermost shell, whereas Ru has four unpaired electrons. Therefore, Ru has more density of states of empty orbitals above the Fermi level than Pt, leading to a stronger adsorption of reaction intermediates during catalysis. The *d*-band center for fcc-Pt (111) and hcp-Ru (0001) surfaces (the most stable facet for Pt and Ru, respectively) further confirms these assumptions. The *d*-band center of Pt is approximately −2.25 eV and Ru is −1.41 eV. This result verifies that Ru exhibits stronger adsorption of intermediates than Pt. To enable Ru to demonstrate Pt-like hydrogen adsorption properties, inject electrons into the vacant orbitals of Ru is a viable strategy. The electron injection shifts a part of electronic states of Ru below the Fermi level, thereby weakening the Ru-H bonds and promoting the hydrogen desorption.

Based on the above conclusions, researchers have employed various strategies such as alloying, constructing heterojunction, doping, and combining with supports to control

hydrogen adsorption free energy, aiming to achieve optimal adsorption energy and improve the HER performance.

### 3.2.1. Alloying and Constructing Heterojunction

Wu et al. [33] prepared RuBi SAA/Bi@OG electrocatalysts by incorporating Bi-doped Ru particles on graphene, resulting in excellent alkaline HER performance. X-ray photoelectron spectroscopy (XPS) and X-ray absorption spectroscopy (XAS) confirmed the electrons transfer from Bi and graphene to Ru particles, which was further supported by DFT simulations through charge density difference and Bader charge calculations (Figure 1a–c). Experimental and theoretical evidence showed that electrons transfer from Bi and graphene to Ru particles successfully weakened hydrogen adsorption on the Ru particle surface. In addition to electron transfer, shortening the Ru–Ru bond length and enhancing the  $d$ – $d$  orbital interactions between Ru atoms can weaken the adsorption of H. Huang et al. [34] synthesized RuCu snowflake-shaped nanosheets (NSs) with enriched channels, which improved the issue of strong Ru hydrogen adsorption (Figure 1d), bringing  $\Delta G_{H^*}$  closer to 0 eV. The Tafel slope in acidic conditions indicated that the HER process followed the Volmer–Tafel pathway, with hydrogen intermediate recombination as the rate-determining step. The hydrogen adsorption free energy close to 0 eV favored the adsorption and desorption of hydrogen at active sites, promoting active sites fast release and accelerating the acidic HER process. RuCu NSs/C-250 °C exhibited satisfactory electrocatalytic water splitting performance, with potentials as low as 1.49, 1.55, 1.9, and 1.50 V at current densities of 10 mA cm<sup>-2</sup> in 1.0 M KOH, 0.1 M KOH, 0.5 M H<sub>2</sub>SO<sub>4</sub>, and 0.05 M H<sub>2</sub>SO<sub>4</sub>, respectively. Furthermore, the optimized RuCu NSs/C-250 °C showed excellent stability in 1.0 M KOH for 45 h. Shi et al. [35] achieved efficient hydrogen evolution by constructing a Schottky junction Ru-WO<sub>2.72</sub> [36]. The resulting Ru-WO<sub>2.72</sub> had a flower-like spherical morphology composed of WO<sub>2.72</sub> nanowires. The electron composition at the interface between metal and metal oxide in Ru-WO<sub>2.72</sub> enhanced the local electron density of Ru, promoting hydrogen activation and accelerating the HER process [37]. The prepared composite material with low Ru loading (2.73 wt%) achieved a 40 mV overpotential at 10 mA cm<sup>-2</sup> (Figure 1e). Ru-WO<sub>2.72</sub> showed stability in 0.5 M H<sub>2</sub>SO<sub>4</sub> for 10 h. The synergistic effect between Ru and WO<sub>2.72</sub>, along with the electron transfer from WO<sub>2.72</sub> to Ru, enriching the electron-rich Ru surface and enhancing the HER performance (Figure 1f–h).

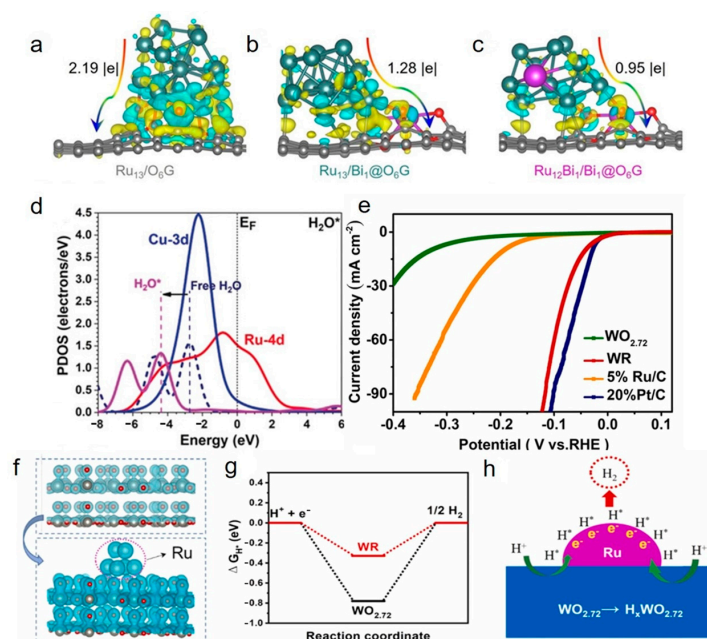


**Figure 1.** The mechanism of enhancing HER performance and HER performance of Ru-based catalysts with modification. (a–c) charge density difference image of Ru<sub>13</sub>/O<sub>6</sub>G, Ru<sub>13</sub>/Bi<sub>1</sub>@O<sub>6</sub>G and

Ru<sub>12</sub>Bi<sub>1</sub>/Bi<sub>1</sub>@O<sub>6</sub>G, respectively; (d) partial density of states (PDOS) analysis for H<sub>2</sub>O adsorption on RuCu nanosheets (NSs); (e) linear sweep voltammetry (LSV) curves comparing the electrocatalytic activity of WO<sub>2.72</sub>, WR, Ru/C, and Pt/C; (f) charge density difference between WO<sub>2.72</sub> (top) and WR (bottom); (g) free energy diagram on the (010) plane of WR and WO<sub>2.72</sub>; (h) schematic representation illustrating the HER mechanism on the WR catalyst. Reproduced from [33–35]. Copyright © John Wiley and Sons, 2023; 2019; Elsevier, 2022.

### 3.2.2. Doping and Combining with Supports

According to DFT calculations, introducing Ru into the NiCo can accelerate the rate of water dissociation, optimize H adsorption–desorption and enhancing alkaline HER activity. Huang et al. [38] designed a series of NiCoRu<sub>x</sub>/SP catalysts based on DFT calculation and found that increasing Ru doping led to a gradual decrease in NiCo surface water dissociation energy barrier from 0.7 eV to 0.3 eV (Figure 2a), which accelerated the Volmer process and optimized the adsorption and desorption of H on the Ru-Ni/Co interface. Ru as the hydrogen evolution active site in NiCoRu<sub>x</sub>/SP catalysts is significant. The NiCoRu<sub>0.2</sub>/SP electrocatalyst, with the most suitable Ru doping amount, achieved a 59 mV overpotential at 10 mA cm<sup>-2</sup> in the 1 M KOH electrolyte. And it can stay stability for 100 h. Excessive Ru doping (NiCoRu<sub>0.3</sub>/SP) led to a strong  $\Delta G_{H^*}$  and decrease HER performance. X-ray absorption spectroscopy and additional characterizations provide further evidence that excessive Ru incorporation leads to a decrease in HER efficiency due to the formation of Ru cluster at the interface between Ru atom and Ni/Co.

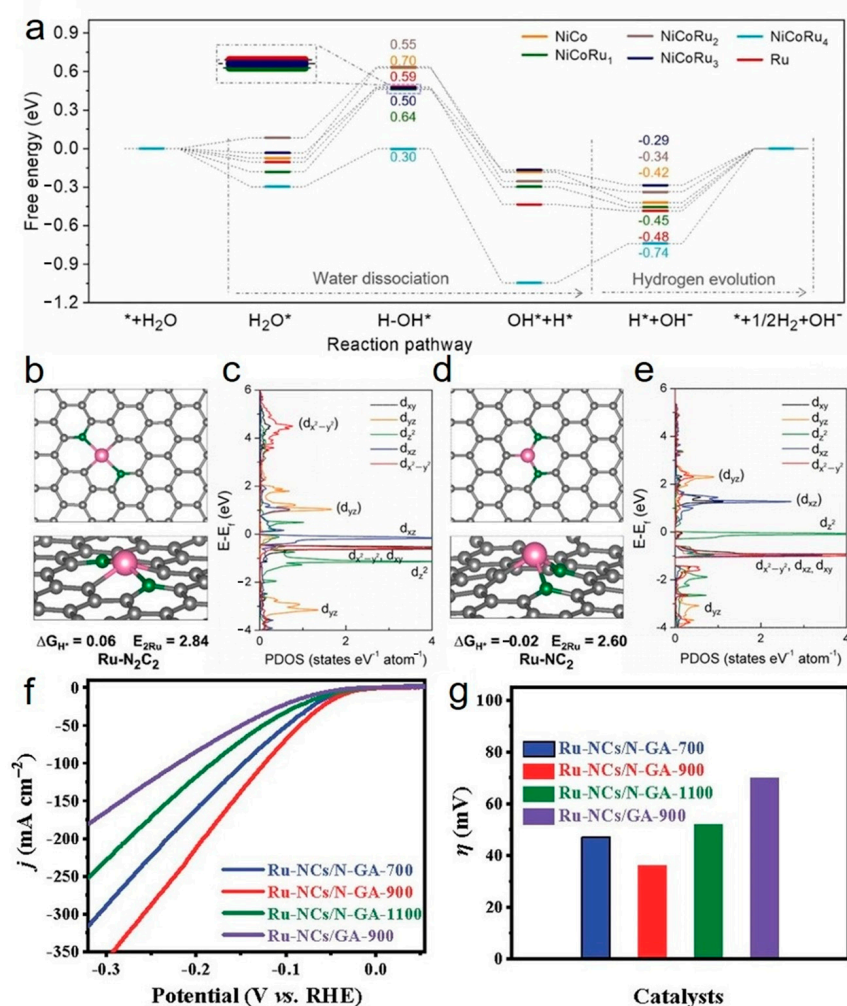


**Figure 2.** HER enhancement mechanism and HER performance of Ru-based catalysts. (a)  $\Delta G_{H^*}$  of HER on the surfaces of NiCoRu<sub>x</sub> along the pathway including water dissociation and hydrogen

desorption; (b)  $\Delta G_{H^*}$  of Ru sites embedded on a  $N_2C_2$  site ( $Ru-N_2C_2$ ); (c) the PDOS of Ru sites embedded on a  $N_2C_2$  site ( $Ru-N_2C_2$ ); (d)  $\Delta G_{H^*}$  of Ru sites embedded on a  $N_2C$  site ( $Ru-N_2C$ ); (e) the PDOS of Ru sites embedded on a  $N_2C$  site ( $Ru-N_2C$ ); (f,g) electrochemical performance of the Ru-NCs/N-GA-700, Ru-NCs/N-GA-900, Ru-NCs/N-GA-1100, and Ru-NCs/GA-900 nano-composites and commercial 20 wt% Pt/C electrocatalyst in  $N_2$ -saturated 1 mol/L KOH electrolyte; (f) LSV curves; (g)  $\eta_{10}$  values. Reproduced from [38–40]. Copyright © Elsevier, 2023; John Wiley and Sons, 2019; Elsevier, 2022.

Furthermore, carbon supports are frequently employed to modulate the electronic distribution of catalysts due to the electron-rich structure. This strategy enables the adjustment of electron density of Ru, resulting in favorable Ru-H adsorption energies. Tiwari et al. [39] achieved exceptional HER performance and remarkable stability by implanting Ru singleatoms and ruthenium nitride nanoparticles on N-doped graphene nanosheets, thus creating an electrocatalyst denoted as  $Ru@RuN_x@GN/C_3N_4-GN$ . This electrocatalyst exhibited outstanding HER activity in both acidic and alkaline environments. In acidic media (0.5 M  $H_2SO_4$ ), the catalyst demonstrated an overpotential as low as 10 mV at a current density of  $10 \text{ mA cm}^{-2}$ , surpassing the performance of commercial Pt/C catalysts. In alkaline media (1.0 M KOH), it achieved an overpotential of only 7 mV at a current density of  $10 \text{ mA cm}^{-2}$  and maintained stability for 150 h in a membrane electrode assembly setup in the acidic solution. DFT calculations revealed that single ruthenium atom sites exhibit near 0 eV  $\Delta G_{H^*}$  values (Figure 2b–e).

The integration of precious metal single atoms with carbon supports not only reduces the consumption of precious metals, but also maximizes the utilization of precious metal single atoms, improving the mass activity. Chen et al. [40] employed nitrogen-doped graphene as the support to incorporate Ru nanoclusters into a networked structure, producing a Ru-based three-dimensional graphene oxide aerogel composite through an adsorption–thermal decomposition method [41]. The electron-rich character of nitrogen-doped graphene accelerated electron transfer, lowering the hydrogen adsorption free energy on Ru sites, promoting H adsorption–desorption, and exposing more active sites, facilitating mass transport. In alkaline conditions, an overpotential of only 36 mV at a current density of  $10 \text{ mA cm}^{-2}$  was achieved (Figure 2f,g), with a low Tafel slope of  $37.8 \text{ mV dec}^{-1}$ . And it can stay stability for 40 h in 1.0 M KOH at  $10 \text{ mA cm}^{-2}$ .

### 3.2.3. Other Modification Examples

Huang et al. [42] proposed a solvent-thermal method to fabricate ultrathin RuZn nanosheets (NSs) with a unique structure characterized by a Moire superlattice and abundant edges. Due to the special structure, the RuZn NSs catalyst, without the Moire superlattice (RuZn NSs–AS), exhibited a superior HER activity across the wide pH range compared to Ru NSs and RuZn NSs. DFT calculations indicated that the anchoring of Zn on Ru NSs shifts the *d*-band center of Ru downward, weakening the Ru–H bond (Figure 3a) and reducing the dissociation energy barrier of water. This design results in a highly efficient and cost-effective pH-universal HER electrocatalyst.

Additionally, the transport of byproduct  $OH^-$  in neutral/alkaline HER significantly influences the HER, because the strong adsorption of  $OH_{ad}$  can lead to catalyst poisoning. The excessive binding of  $OH_{ad}$  to active sites prevents the fast release, ultimately resulting in a decline of HER performance. Feng et al. [43] introduced an approach that combine  $SnO_2$  with Ru single atom to address the issue of excessive  $OH_{ad}$  adsorption.  $OH_{ad}$  served as the harmful intermediate in the HER process. The strong interaction between Ru and  $OH_{ad}$  led to the occupation of active sites. This phenomenon, known as poisoning of Ru single-atom sites, substantially diminished HER activity.  $SnO_2$  exhibited an affinity for oxygen that  $OH_{ad}$  predominantly bound to  $SnO_2$  when HER occurs, allowing that the active sites of Ru single atoms are accessible (Figure 3b). This effect contributed to the enhancement of HER performance. Furthermore, Sun et al. [44] loaded different-sized Ru catalysts (single atoms, nanoclusters, and nanoparticles) on N-doped carbon (NC) [45]

support (Figure 3c), preparing a pH-universal Ru-based electrocatalyst. Among these catalysts, Ru nanocluster catalysts (Ru NCs/NC) exhibited the best catalytic performance, with overpotentials of only 14, 30, and 32 mV (at a current density of  $10 \text{ mA cm}^{-2}$ ) in 1.0 M KOH, 1.0 M phosphate-buffered saline (PBS), and 0.5 M  $\text{H}_2\text{SO}_4$ , respectively. And it can maintain the stability for 50 h in 1.0 M KOH at  $10 \text{ mA cm}^{-2}$ . DFT calculations revealed that strong interactions between Ru nanoclusters and N-doped carbon carriers resulted in a downward shift of the *d*-band center, weakening the  $\text{H}^*$  adsorption on Ru sites, making it more favorable for adsorption and desorption [46–49].

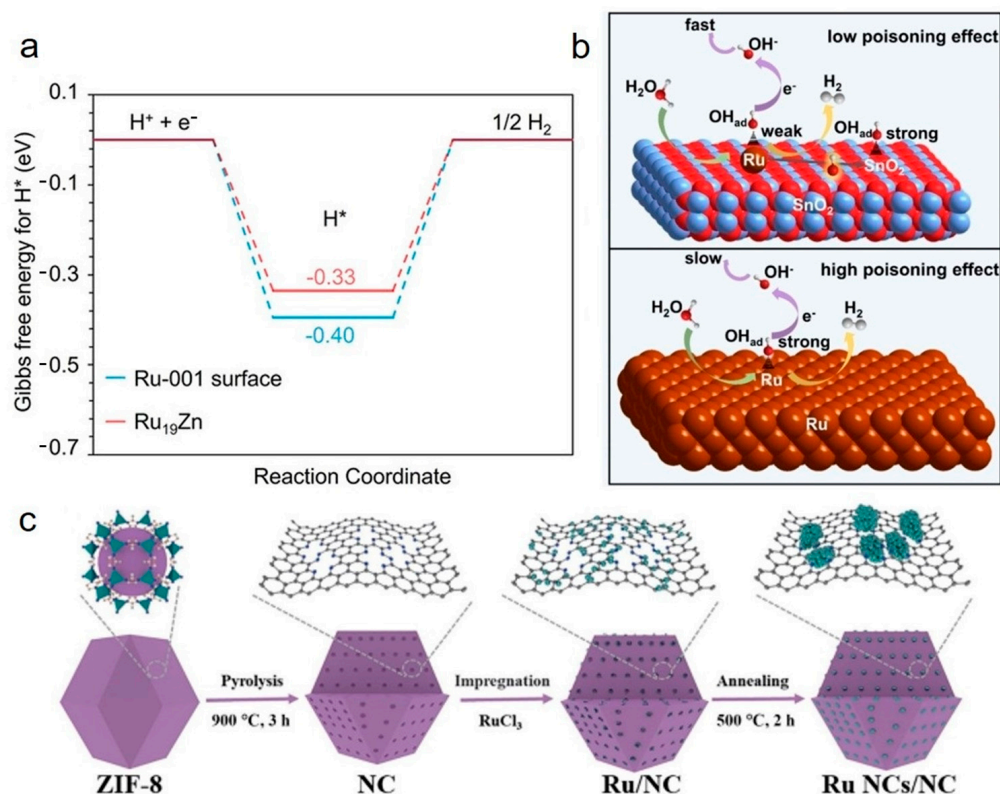


**Figure 3.** The mechanism of Ru-based catalysts to improve HER performance. (a) Comparison of the Gibbs free energy for hydrogen adsorption ( $\text{H}^*$ ) on the Ru-001 surface and  $\text{Ru}_{19}\text{Zn}$ -001; (b) schematic of HER mechanism on Ru SAs-SnO<sub>2</sub>/C; (c) schematic diagram showing the synthesis of Ru NCs/NC. Reproduced from [42–44]. Copyright © John Wiley and Sons, 2023; 2022; Springer Nature, 2023.

#### 4. Water Molecule Adsorption and Activation

The adsorption–activation–cleavage of water molecules on the catalyst surface is vital for neutral/alkaline HER. In typical electrocatalytic HER catalysts, the energy barrier of water molecule cleavage is often higher than that of hydrogen desorption. This indicates that the water molecule cleavage step is the rate-limiting step in neutral/alkaline HER. Generally, water molecules are more likely to cleavage when they are strongly adsorbed on active sites. This is because the strong electronic interaction between water molecules and active sites weakens the electronic interaction within the H–O bonds of water molecules, thus increasing the possibility of water molecule cleavage.

##### 4.1. Adsorption and Activation of $\text{H}_2\text{O}$

The molecular orbital of  $\text{H}_2\text{O}$  is depicted (Figure 4). Typically, the adsorption configuration of  $\text{H}_2\text{O}$  on the surface of transition metal catalysts involves the binding of the oxygen atom in water molecules to metal sites. The adsorption primarily occurs through the coordination of the lone pair electrons on the oxygen atom with the vacant orbitals in the metal. These lone pair electrons on oxygen atoms exist in the highest occupied molecular orbital

(HOMO) of H<sub>2</sub>O. When the HOMO electrons shift towards the metal site, the Fermi level of the H<sub>2</sub>O shifts downward, which results in an increased possibility of electron loss from the HOMO-1 orbital, the H-O  $\sigma$ -bonding orbital. This makes the activation of the H-O bond more favorable, leading to the cleavage of H<sub>2</sub>O. It is important to note that the strength of water molecule adsorption and the cleavage are directly correlated. Furthermore, the abundance and types of vacant orbitals available for water coordination in the catalyst are directly linked to the adsorption and cleavage of water molecules. This information provides a basis for the rational design of water adsorption–cleavage sites in HER catalysts.

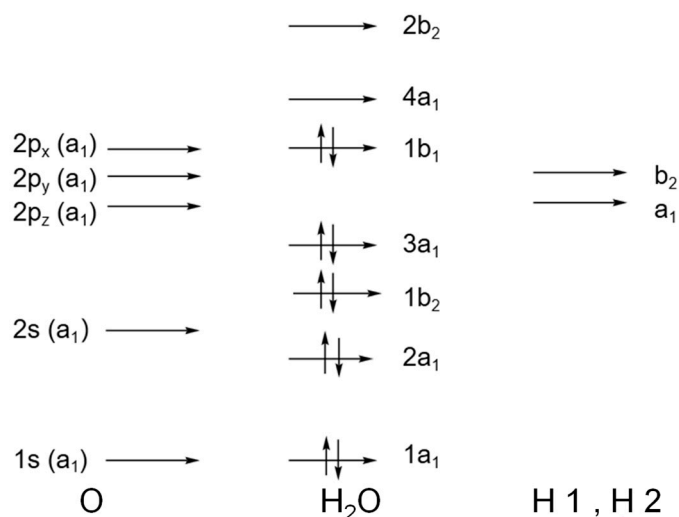


**Figure 4.** Energy level diagram of water molecular orbitals.

#### 4.2. Strengthening the Adsorption and Activation of Interfacial Water Molecules

Researchers have made significant efforts to improve the adsorption and cleavage of H<sub>2</sub>O. Introducing transition metals on the catalyst surface is an effective strategy. Many materials have shown promise in neutral/alkaline HER, such as Ru-Mn alloys, Ru-Mo alloys, and Cu-doped Ru/RuSe<sub>2</sub>. Additionally, Ru-Bi alloys and Ru single atoms dispersed on carriers have demonstrated satisfactory neutral/alkaline HER performance [50].

Guo et al. [51] synthesized Cu-doped heterogeneous Ru/RuSe<sub>2</sub> nanosheets with the solution-phase method. The nanosheets exhibited a low overpotential of 23 mV at 10 mA cm<sup>-2</sup>, with a Tafel slope of 58.5 mV dec<sup>-1</sup> and a turnover frequency (TOF) of 0.88 s<sup>-1</sup>. And it showed no attenuation after 5000-cycles accelerated durability tests. DFT calculations investigated the electronic structure of the heterogeneous interface. Due to the unique heterogeneous interface structure and a synergistic effect with Cu doping, it led to an electron structure with suitable d-band centers (Figure 5a), thereby reducing  $\Delta G_{H^*}$ . Furthermore, it enhanced the adsorption of H<sub>2</sub>O, accelerated H<sub>2</sub>O dissociation, and simultaneously lowered the barrier, thereby improving HER performance. Huang et al. [52] designed and synthesized ultrathin Mn-doped Ru nanosheet branches (RuMn NSBs) by using the wet chemical approach. In 1.0 M KOH electrolyte, RuMn NSBs-250 exhibited an overpotential of 20 mV at 10 mA cm<sup>-2</sup>, lower than that of commercial Pt/C (44 mV) and Ir/C (51 mV). The charge transfer resistance ( $5.1 \pm 0.06 \Omega \text{ cm}^2$ ) in RuMn NSBs-250 was smaller than that of commercial Pt/C ( $9.8 \pm 0.1 \Omega \text{ cm}^2$ ) and Ir/C ( $24.4 \pm 0.3 \Omega \text{ cm}^2$ ), indicating the faster electron transfer efficiency in RuMn NSBs-250. DFT calculations showed that the addition of Mn altered the electronic structure. The *d*-*d* coupling between Ru and nearby Mn resulted in more electron density near the Fermi level (Figure 5b), accelerating electron transfer on the RuMn NSB surface and improving water dissociation performance. Mu et al. [53] synthesized a hollow octahedral Ru-Cu-MoO<sub>2</sub>, in which Ru and Cu-MoO<sub>2</sub> existed as clusters and nanocrystals, respectively. Under alkaline-pH, acidic-pH, and alkaline seawater conditions, the overpotentials were 22, 48, and 23 mV at 10 mA cm<sup>-2</sup>, respectively. And it can maintain the stability for 25 h at 10 mA cm<sup>-2</sup> in

1.0 M KOH. Moreover, DFT calculations further demonstrated that Ru-Cu-MoO<sub>2</sub> [54] had the best  $\Delta G_{H^*}$  values and appropriate water adsorption energies (Figure 5c), lowering the kinetic energy barrier of HER. Che et al. [55] reported a simple one-step pyrolysis method to synthesize uniformly dispersed ultrafine Ru nanocrystals on N-doped carbon (Ru/NC) as an electrocatalyst for alkaline-pH HER. DFT calculations confirmed its superior HER performance. This showed that Ru/NC had lower water dissociation barriers compared to Ru, and it achieved the optimal  $\Delta G_{H^*}$  (Figure 5d). Zhou et al. [56] successfully dispersed Ru single atoms into N-doped Mo<sub>2</sub>C nanosheets by using the Ostwald ripening strategy. Ru SAs/N-Mo<sub>2</sub>C NSs demonstrated HER activity, with an overpotential of 43 mV (at 10 mA cm<sup>-2</sup>) in 1.0 M KOH. In 1.0 M KOH, Ru SAs/N-Mo<sub>2</sub>C NSs exhibited stability for HER, with only a 3.7% attenuation over 8 h and 6.3% over 60 h at an overpotential of 100 mV. The performance significantly outperformed that of Ru NPs/Mo<sub>2</sub>C NSs, which experienced a 32.3% attenuation over 8 h. DFT calculations demonstrated significant interface synergies between Ru SAs and N-Mo, accelerating H<sub>2</sub>O dissociation and optimizing  $\Delta G_{H^*}$  in alkaline-pH condition (Figure 5e,f).

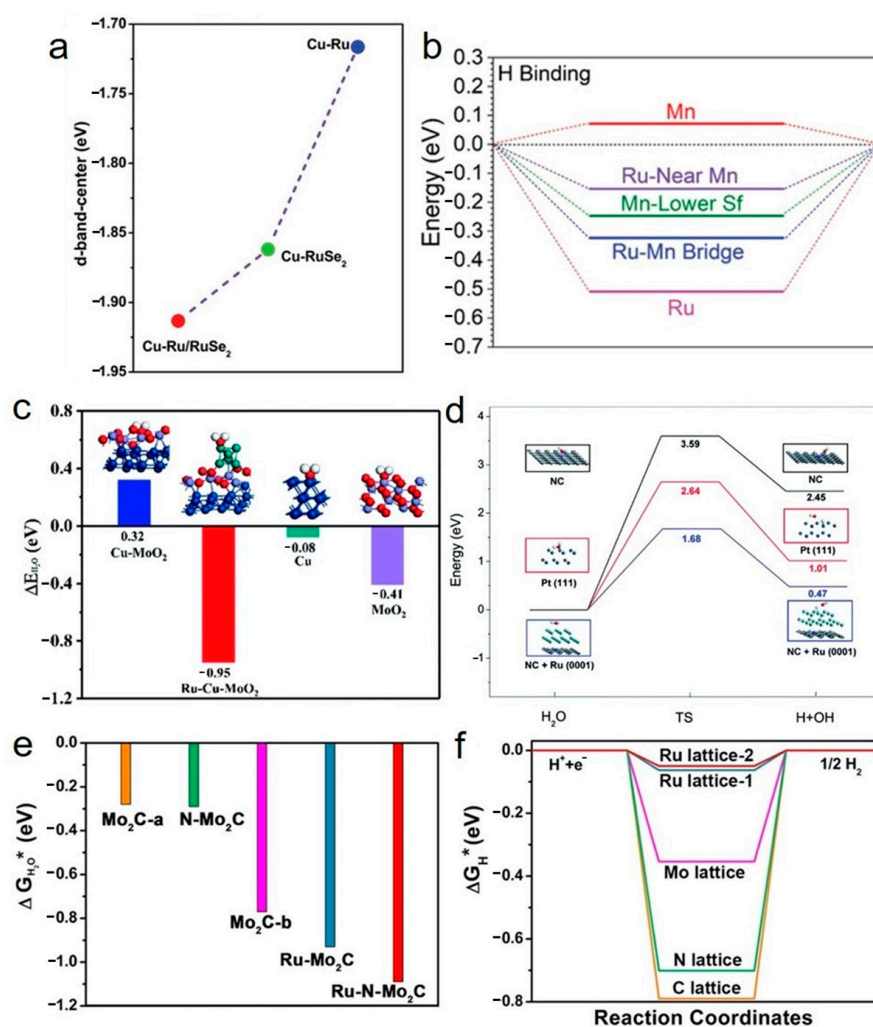


**Figure 5.** Free energy regulation of Ru-based modified materials. (a) The d-band center changes in Cu-doped Ru/RuSe<sub>2</sub>; (b) H binding energy at different sites of RuMn NSBs; (c) water adsorption energies of Cu, MoO<sub>2</sub>, Cu-MoO<sub>2</sub> and Ru-Cu-MoO<sub>2</sub>; (d) computed reaction barriers and pathways for the Volmer step on various surfaces, revealing the impact of surface modifications on reaction kinetics; (e) adsorption free energies of H<sub>2</sub>O; (f) free energies of H adsorption in different configurations. Reproduced from [51–53,55,56]. Copyright © John Wiley and Sons, 2023; 2021; Royal Society of Chemistry, 2022; 2019; Elsevier, 2020.

Due to strict requirements and limitations on the corrosion resistance of devices and catalysts imposed by acidic oxygen evolution reaction (OER), significant attention has been directed towards alkaline and neutral water electrolysis for hydrogen production in recent years. In contrast to acidic HER, where protons serve as the reactants,  $\text{H}_2\text{O}$  is the primary reaction species in alkaline and neutral electrolytes. So, additional steps are required involving water molecule activation and cleavage. To enhance the efficiency of Ru-based catalysts, the introduction of additional water molecule activation and cleavage sites within the catalyst structure has proven to be an effective strategy. The key to efficiently activating and cleaving water molecules lies in the strong electronic–orbital interactions between active sites with water molecules. This is generally achieved by coordination between the active sites and oxygen atoms in the water molecules, directly improving the interaction between Ru and O. However, strengthening the Ru–O interaction can also lead to increased Ru–H interactions, which are unfavorable for the rapid progression of the hydrogen desorption step. Therefore, a viable strategy is to directly combine oxygen-attractive materials with Ru catalysts to address this challenge effectively. Wang et al. [57] prepared the  $\text{Ru-WO}_{3-x}$  catalyst by loading Ru nanoparticles on the  $\text{WO}_3$  surface rich in oxygen vacancies. Tungsten (W), as an early transition metal, exhibited fewer valence electrons, providing an abundance of vacant orbitals available for O coordination (Figure 6a). Furthermore, the formation of oxygen vacancies on the  $\text{WO}_3$  surface was produced by the  $\text{H}_2$  reduction process. The innovative catalyst demonstrated exceptional electrocatalytic performance for HER in neutral electrolytes (Figure 6b). The oxygen vacancies enhanced the coordination between W and oxygen atoms within  $\text{H}_2\text{O}$  (Figure 6c).

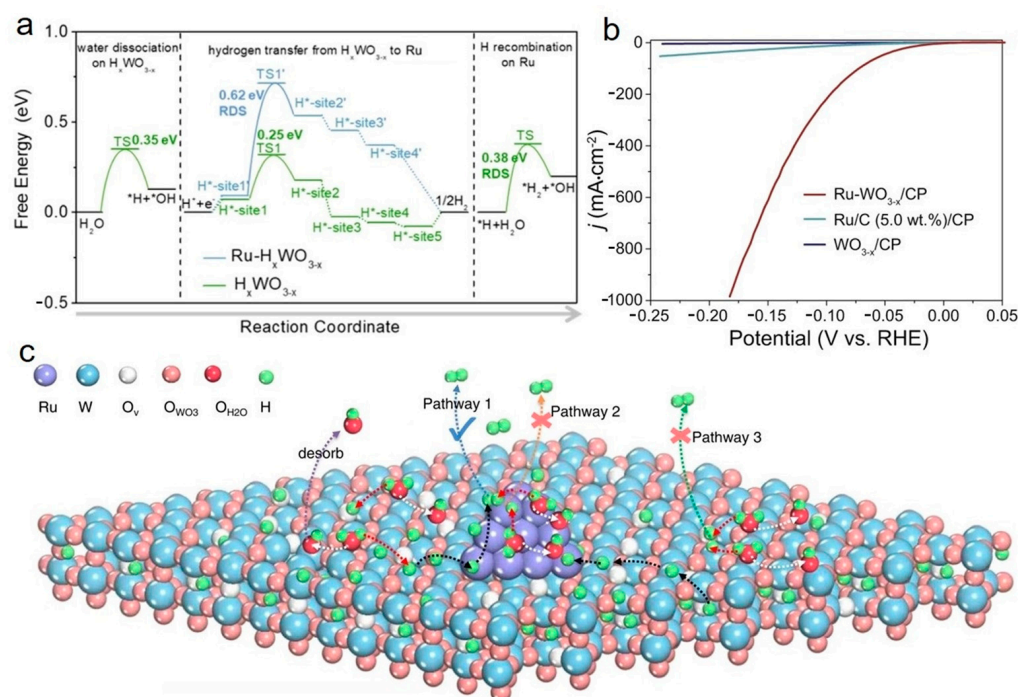


**Figure 6.** HER performance and mechanism of  $\text{Ru-WO}_{3-x}$ . (a) Calculated free energy diagram for HER on  $\text{Ru-H}_x\text{WO}_{3-x}$  and  $\text{H}_x\text{WO}_{3-x}$ ; (b) LSV curves in 1.0 M PBS; (c) illustration of hydrogen spillover. Reproduced under the terms of the CC-BY Creative Commons Attribution 4.0 International license (<http://creativecommons.org/licenses/by/4.0/>, accessed on 18 October 2023) [57].

## 5. Interfacial Water Behavior in HER

The behavior of interfacial water is a significant scientific issue in catalytic processes, although it is frequently overlooked [58]. Interfacial water molecules represent only a small part of the entire reaction system, and they do not directly adsorb onto the surface of catalyst. Instead, they influence the mass transport in the reaction, making it challenging to directly observe the motion of interfacial water molecules using conventional electrochemical

testing methods and characterization techniques. Furthermore, theoretical simulations face limitations in simulating electrochemical polarization with difficulty and small simulation scale. In recent years, with the rapid development of in situ characterization techniques and Ab initio molecular dynamics (AIMD) simulation, there has been a growing interest in investigating the behavior of H<sub>2</sub>O at the electrocatalytic interfaces.

### 5.1. The Mechanism of Interfacial Water Behavior

In HER, interface water serves not only as a reactant but also as the reaction environment. Consequently, understanding the behavior of interface water in HER is important for the rational design of catalysts and reaction systems. In general, HER requires catalyst surfaces to possess high hydrophilicity and low gas affinity. Firstly, enhancing the hydrophilic nature of the surface facilitates the rapid departure of generated hydrogen bubbles from the material surface. This improved contact between the reactants with catalytic active sites, increasing the turnover frequency of the catalytic active sites. Secondly, a hydrophilic surface reduces the adhesion between hydrogen bubbles and the catalyst, enabling bubbles to detach from the surface when they reach a smaller size. This prevents the bursting of large hydrogen bubbles, preserving the structural integrity of the catalyst and enhancing its stability. Finally, hydrophilic catalyst surfaces typically exhibit higher mass transfer efficiency, and the byproduct OH<sup>−</sup> can rapidly depart from the surface. This increases the possibility of reactant collisions with active sites, ultimately elevating the turnover frequency of catalytic active sites. To enhance the hydrophilic nature of catalyst surfaces and consequently, catalytic efficiency and stability, methods such as constructing micro-nano hierarchical structures, using hydrophilic materials for modification, and altering surface polarity have proven effective.

Creating hydrophilic surfaces serves as a strategy for enhancing mass transfer and improving the conversion frequency of active sites on a larger scale, ranging from micrometers to millimeters. However, the behavior of interfacial water molecules, including their configuration and orientation, is equally significant on the atomic scale. In contrast to acidic-pH HER, hydrogen bonding between water molecules strengthens with the pH increasing, resulting in a more rigid catalyst-interface water. The rigidity limits the diffusion of generated byproducts like OH<sup>−</sup> in the solution, making it challenging to renew catalytic active sites and resulting in a decrease in the conversion frequency of active sites. To reduce hydrogen bonding among interfacial water molecules and make them more “flexible”, researchers have adopted strategies such as surface modification, the construction of heterostructures [59], and the introduction of additives into the system. They have also utilized in situ spectroscopy and AIMD to investigate the behavior of interfacial water in catalysts and summarize the principles.

### 5.2. Research on Interface Water Behavior

Due to the unique surface properties of Ru, which neither exhibits a strong affinity for hydrogen like O or N sites nor a pronounced preference for oxygen like Mo or V sites, water molecules on the surface of Ru do not adopt a clear H-down or O-down configuration. This leads to a situation where the surface of Ru is not favorable for either hydrogen evolution or water splitting. To enhance the efficiency of water molecule cleavage, the introduction of pre-transition metals on the catalyst surface can render it more oxygen friendly, promoting the O-down configuration of H<sub>2</sub>O and improving water splitting efficiency. Similarly, introducing species like O, S, Se, or N on the surface to make it more hydrogen friendly and promote the H-down configuration has proven to be an effective strategy.

Li et al. [60] made significant contributions to the study of interfacial water behavior of HER using in situ Raman spectroscopy. Ru demonstrates comparable or superior activity to Pt in HER. However, the mechanistic understanding remains unresolved. They found that dynamic spectral evidence of Ru surfaces, interfacial water, \*H, and \*OH intermediates is simultaneously captured. Ru surfaces, existing in different valence states within the reaction potential range, dissociate interfacial water differently, generating two distinct \*H

species with varying activities. The local cation tuning effect of hydrated  $\text{Na}^+$  ions and the high work function of high-valence  $\text{Ru}(n^+)$  surfaces promote interfacial water dissociation. Additionally, high-valence  $\text{Ru}(n^+)$  surfaces exhibit more moderate adsorption energies for interfacial water,  $^*\text{H}$ , and  $^*\text{OH}$  compared to low-valence  $\text{Ru}(0)$  surfaces, enhancing catalytic activity. These findings highlight the regulatory role of valence state in interfacial water, intermediates, and catalytic activity, providing guidelines for the rational design of highly efficient catalysts. Chen et al. [61] constructed heterogeneous structures, such as  $\text{Ru-N/C}$  and  $\text{RuSe}_x$ , utilizing the strong attraction of Se to H to disrupt the interfacial water network in the catalyst. The disruption led to the formation of the H-down configuration among interfacial water molecules (Figure 7c,d), reducing hydrogen bonding, decreasing the rigidity of the interfacial water, and enhancing mass transfer efficiency.  $\text{Ru-N/C}$  single-atom sites effectively served as H adsorption–desorption sites to efficiently catalyze hydrogen evolution.

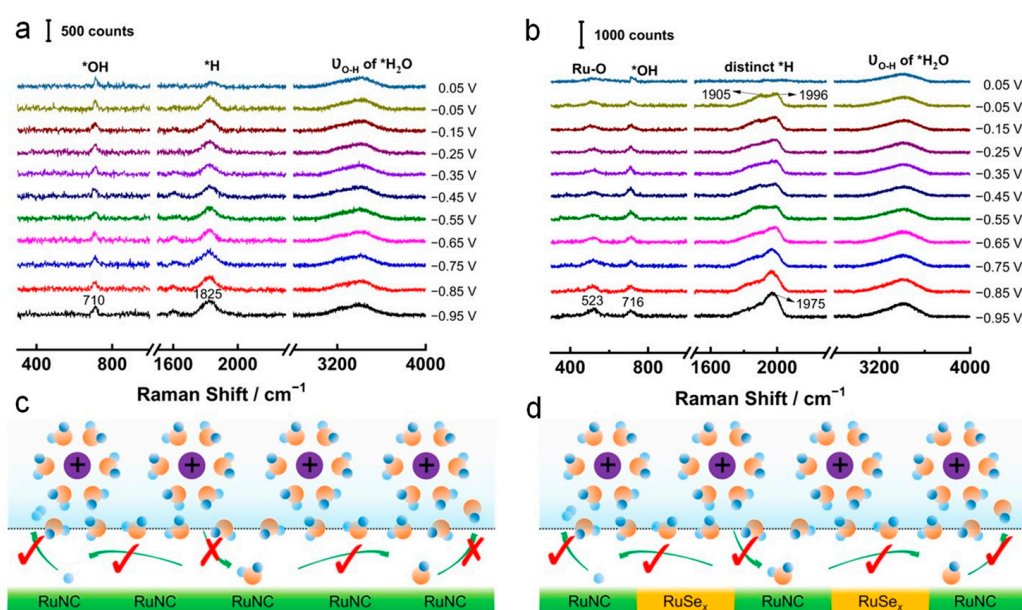


**Figure 7.** Water behavior of Ru sites in materials. In situ Raman spectra and the corresponding HER performance at Ru surfaces in different valence states. (a) At  $-0.95$  V for reduction for 30 min; (b) at  $+0.95$  V for oxidation for 20 min; (c) proposed mechanisms for neutral HER over  $\text{RuNC}$ ; (d) proposed mechanisms for neutral HER over  $\text{RuSe}_x\text{-RuNC}$ . Reproduced under the terms of the CC-BY Creative Commons Attribution 4.0 International license (<http://creativecommons.org/licenses/by/4.0/>), accessed on 18 October 2023) [60,61].

## 6. The Future Perspective

Currently, while Ru-based catalysts are considered one of the most promising HER catalysts as a cost-effective alternative to Pt, research on Ru-based catalysts is far from adequate. Challenges persist, hindering their widespread application. The issues include the high cost and limited abundance of Ru, as well as stability concerns under harsh electrolysis conditions. To address these challenges, innovative strategies encompassing catalyst design with earth-abundant materials and surface modifications for enhanced stability are proposed.

Additionally, existing studies have primarily focused on intermediate adsorption, optimizing the adsorption of intermediates by adjusting electron density. However, the structure and adsorption behavior of interface water molecules also have a significant impact on HER performance, and research on interface water behavior is still relatively limited. Most studies have only involved the surface of understanding how intermediates adsorb and desorb, how their states change during the HER process, and the behavior of interface water molecules. In-depth exploration of the HER mechanism can be achieved

through the use of a range of in situ characterization technologies, such as in situ Raman spectroscopy and TEM.

In a word, H<sub>2</sub> has significant promise in addressing issues such as environmental pollution, greenhouse gas emissions, and energy scarcity [62–64]. The development and utilization of hydrogen energy are still at the initial stages, with researchers continuing to research deeper into the transition from industrial-scale production to practical application [65]. In this review, recent advances in enhancing the efficiency of Ru-based catalysts for water electrolysis and H<sub>2</sub> production have been summarized, focusing on the mechanisms of HER, including the adsorption of intermediates on catalyst surfaces, the adsorption and activation of interface water molecules, and the behavior of interface water molecules. This review hopes to provide researchers with new insights for the deeper design and modification of Ru-based catalysts by summarizing the research progress of Ru-based catalysts from a mechanism perspective. Ultimately, it will contribute to the development of highly efficient, cost-effective catalysts that can find widespread industrial application [66,67] in the future.

**Author Contributions:** L.L. searched the literature, and wrote the main part of the current work; F.T. contributed with data analysis, writing and revision of the current literature; L.Q. and F.W. wrote part of this work; W.Y. and Y.Y. organized, supervised and reviewed this work. All authors have read and agreed to the published version of the manuscript.

**Funding:** This work was supported by the National Natural Science Foundation of China under Grant (No. 51871078 and 52071119) and the Heilongjiang Science Foundation (No. LH2020B006).

**Conflicts of Interest:** The authors declare no conflict of interest.

## References

1. Yu, Z.; Duan, Y.; Feng, X.; Yu, X.; Gao, M.; Yu, S. Clean and Affordable Hydrogen Fuel from Alkaline Water Splitting: Past, Recent Progress, and Future Prospects. *Adv. Mater.* **2021**, *33*, 2007100. [[CrossRef](#)] [[PubMed](#)]
2. Yang, Y.; Yu, Y.; Li, J.; Chen, Q.; Du, Y.; Rao, P.; Li, R.; Jia, C.; Kang, Z.; Deng, P.; et al. Engineering Ruthenium-Based Electrocatalysts for Effective Hydrogen Evolution Reaction. *Nano-Micro Lett.* **2021**, *13*, 160. [[CrossRef](#)] [[PubMed](#)]
3. Luo, Y.; Zhang, Z.; Chhowalla, M.; Liu, B. Recent Advances in Design of Electrocatalysts for High-Current-Density Water Splitting. *Adv. Mater.* **2022**, *34*, 2108133. [[CrossRef](#)] [[PubMed](#)]
4. Peng, X.; Xie, S.; Wang, X.; Pi, C.; Liu, Z.; Gao, B.; Hu, L.; Xiao, W.; Chu, P.K. Energy-Saving Hydrogen Production by the Methanol Oxidation Reaction Coupled with the Hydrogen Evolution Reaction Co-Catalyzed by a Phase Separation Induced Heterostructure. *J. Mater. Chem. A* **2022**, *10*, 20761–20769. [[CrossRef](#)]
5. Özhava, D.; Özkar, S. Nanoceria Supported Rhodium(0) Nanoparticles as Catalyst for Hydrogen Generation from Methanolysis of Ammonia Borane. *Appl. Catal. B Environ.* **2018**, *237*, 1012–1020. [[CrossRef](#)]
6. Meaburn, G.M.; Mellows, F.W.; Reiffsteck, A. Production of Hydrogen in the Radiolysis of Methanol Vapour. *Nature* **1964**, *204*, 1301–1302. [[CrossRef](#)]
7. Lee, J.; Ga, S.; Lim, D.; Lee, S.; Cho, H.; Kim, J. Carbon-Free Green Hydrogen Production Process with Induction Heating-Based Ammonia Decomposition Reactor. *Chem. Eng. J.* **2023**, *457*, 141203. [[CrossRef](#)]
8. Tabassum, H.; Mukherjee, S.; Chen, J.; Holiharimanana, D.; Karakalos, S.; Yang, X.; Hwang, S.; Zhang, T.; Lu, B.; Chen, M.; et al. Hydrogen Generation via Ammonia Decomposition on Highly Efficient and Stable Ru-Free Catalysts: Approaching Complete Conversion at 450 °C. *Energy Environ. Sci.* **2022**, *15*, 4190–4200. [[CrossRef](#)]
9. Mukherjee, S.; Devaguptapu, S.V.; Sviripa, A.; Lund, C.R.F.; Wu, G. Low-Temperature Ammonia Decomposition Catalysts for Hydrogen Generation. *Appl. Catal. B Environ.* **2018**, *226*, 162–181. [[CrossRef](#)]
10. Ramprakash, B.; Lindblad, P.; Eaton-Rye, J.J.; Incharoensakdi, A. Current Strategies and Future Perspectives in Biological Hydrogen Production: A Review. *Renew. Sustain. Energy Rev.* **2022**, *168*, 112773. [[CrossRef](#)]
11. Łukajtis, R.; Hołowacz, I.; Kucharska, K.; Glinka, M.; Rybarczyk, P.; Przyjazny, A.; Kamiński, M. Hydrogen Production from Biomass Using Dark Fermentation. *Renew. Sustain. Energy Rev.* **2018**, *91*, 665–694. [[CrossRef](#)]
12. Wu, Y.; Ghalkhani, M.; Ashrafzadeh Afshar, E.; Karimi, F.; Xia, C.; Le, Q.V.; Vasseghian, Y. Recent progress in Biomass-derived nanoelectrocatalysts for the sustainable energy development. *Fuel* **2022**, *323*, 124349. [[CrossRef](#)]
13. Salakkam, A.; Sittijunda, S.; Mamimin, C.; Phanduang, O.; Reungsang, A. Valorization of Microalgal Biomass for Biohydrogen Generation: A Review. *Bioresour. Technol.* **2021**, *322*, 124533. [[CrossRef](#)]
14. Xu, W.; Wang, H. Earth-Abundant Amorphous Catalysts for Electrolysis of Water. *Chin. J. Catal.* **2017**, *38*, 991–1005. [[CrossRef](#)]
15. Iqbal, M.Z.; Zahid, R.; Khan, M.W.; Shaheen, M.; Aziz, U.; Aftab, S. Exploration of Catalytically Active Materials for Efficient Electrochemical Hydrogen and Oxygen Evolution Reactions. *Int. J. Hydrog. Energy* **2023**, *48*, 8045–8070. [[CrossRef](#)]

16. Jiang, T.; Liu, Z.; Yuan, Y.; Zheng, X.; Park, S.; Wei, S.; Li, L.; Ma, Y.; Liu, S.; Chen, J.; et al. Ultrafast Electrical Pulse Synthesis of Highly Active Electrocatalysts for Beyond-Industrial-Level Hydrogen Gas Batteries. *Adv. Mater.* **2023**, *35*, 2300502. [[CrossRef](#)] [[PubMed](#)]
17. Tian, W.; Zhang, X.; Wang, Z.; Cui, L.; Li, M.; Xu, Y.; Li, X.; Wang, L.; Wang, H. Amorphization Activated RhPb Nanoflowers for Energy-Saving Hydrogen Production by Hydrazine-Assisted Water Electrolysis. *Chem. Eng. J.* **2022**, *440*, 135848. [[CrossRef](#)]
18. Cui, Z.; Jiao, W.; Huang, Z.; Chen, G.; Zhang, B.; Han, Y.; Huang, W. Design and Synthesis of Noble Metal-Based Alloy Electrocatalysts and Their Application in Hydrogen Evolution Reaction. *Small* **2023**, *19*, 2301465. [[CrossRef](#)]
19. Li, D.; Chen, X.; Lv, Y.; Zhang, G.; Huang, Y.; Liu, W.; Li, Y.; Chen, R.; Nuckolls, C.; Ni, H. An Effective Hybrid Electrocatalyst for the Alkaline HER: Highly Dispersed Pt Sites Immobilized by a Functionalized NiRu-Hydroxide. *Appl. Catal. B Environ.* **2020**, *269*, 118824. [[CrossRef](#)]
20. Zhang, C.; Liang, X.; Xu, R.; Dai, C.; Wu, B.; Yu, G.; Chen, B.; Wang, X.; Liu, N. H<sub>2</sub> In Situ Inducing Strategy on Pt Surface Segregation Over Low Pt Doped PtNi<sub>5</sub> Nanoalloy with Superhigh Alkaline HER Activity. *Adv. Funct. Mater.* **2021**, *31*, 2008298. [[CrossRef](#)]
21. Hansen, J.N.; Prats, H.; Toudahl, K.K.; Mørch Secher, N.; Chan, K.; Kibsgaard, J.; Chorkendorff, I. Is There Anything Better than Pt for HER? *ACS Energy Lett.* **2021**, *6*, 1175–1180. [[CrossRef](#)]
22. Kwon, T.; Yu, A.; Kim, S.; Kim, M.H.; Lee, C.; Lee, Y. Au-Ru Alloy Nanofibers as a Highly Stable and Active Bifunctional Electrocatalyst for Acidic Water Splitting. *Appl. Surf. Sci.* **2021**, *563*, 150293. [[CrossRef](#)]
23. Huang, C.; Yu, Y.; Yang, J.; Yan, Y.; Wang, D.; Hu, F.; Wang, X.; Zhang, R.; Feng, G. Ru/La<sub>2</sub>O<sub>3</sub> Catalyst for Ammonia Decomposition to Hydrogen. *Appl. Surf. Sci.* **2019**, *476*, 928–936. [[CrossRef](#)]
24. Li, J.; Tan, Y.; Zhang, M.; Gou, W.; Zhang, S.; Ma, Y.; Hu, J.; Qu, Y. Boosting Electrocatalytic Activity of Ru for Acidic Hydrogen Evolution through Hydrogen Spillover Strategy. *ACS Energy Lett.* **2022**, *7*, 1330–1337. [[CrossRef](#)]
25. Meng, G.; Tian, H.; Peng, L.; Ma, Z.; Chen, Y.; Chen, C.; Chang, Z.; Cui, X.; Shi, J. Ru to W Electron Donation for Boosted HER from Acidic to Alkaline on Ru/WNO Sponges. *Nano Energy* **2021**, *80*, 105531. [[CrossRef](#)]
26. Xu, J.; Chen, C.; Kong, X. Ru-O-Cu Center Constructed by Catalytic Growth of Ru for Efficient Hydrogen Evolution. *Nano Energy* **2023**, *111*, 108403. [[CrossRef](#)]
27. Zhang, X.; He, Y.; Zhu, B.; Wan, X.; Hua, S.; Tang, H. A Bottom-up Method to Construct Ru-Doped FeP Nanosheets on Foam Iron with Ultra-High Activity for Hydrogen Evolution Reaction. *Int. J. Hydrog. Energy* **2023**, *48*, 4686–4693. [[CrossRef](#)]
28. Wang, C.; Shang, H.; Li, J.; Wang, Y.; Xu, H.; Wang, C.; Guo, J.; Du, Y. Ultralow Ru Doping Induced Interface Engineering in MOF Derived Ruthenium-Cobalt Oxide Hollow Nanobox for Efficient Water Oxidation Electrocatalysis. *Chem. Eng. J.* **2021**, *420*, 129805. [[CrossRef](#)]
29. Sun, X.; Gao, X.; Chen, J.; Wang, X.; Chang, H.; Li, B.; Song, D.; Li, J.; Li, H.; Wang, N. Ultrasmall Ru Nanoparticles Highly Dispersed on Sulfur-Doped Graphene for HER with High Electrocatalytic Performance. *ACS Appl. Mater. Interfaces* **2020**, *12*, 48591–48597. [[CrossRef](#)] [[PubMed](#)]
30. Jiang, S.; Suo, H.; Zhang, T.; Liao, C.; Wang, Y.; Zhao, Q.; Lai, W. Recent Advances in Seawater Electrolysis. *Catalysts* **2022**, *12*, 123. [[CrossRef](#)]
31. Li, J.; Zhang, J.; Shen, J.; Wu, H.; Chen, H.; Yuan, C.; Wu, N.; Liu, G.; Guo, D.; Liu, X. Self-Supported Electrocatalysts for the Hydrogen Evolution Reaction. *Mater. Chem. Front.* **2023**, *7*, 567–606. [[CrossRef](#)]
32. Zhou, B.; Gao, R.; Zou, J.; Yang, H. Surface Design Strategy of Catalysts for Water Electrolysis. *Small* **2022**, *18*, 2202336. [[CrossRef](#)]
33. Zhao, X.; Wu, G.; Zheng, X.; Jiang, P.; Yi, J.; Zhou, H.; Gao, X.; Yu, Z.-Q.; Wu, Y. A Double Atomic-Tuned RuBi SAA/Bi@OG Nanostructure with Optimum Charge Redistribution for Efficient Hydrogen Evolution. *Angew. Chem. Int. Ed.* **2023**, *62*, e202300879. [[CrossRef](#)]
34. Yao, Q.; Huang, B.; Zhang, N.; Sun, M.; Shao, Q.; Huang, X. Channel-Rich RuCu Nanosheets for pH-Universal Overall Water Splitting Electrocatalysis. *Angew. Chem. Int. Ed.* **2019**, *58*, 13983–13988. [[CrossRef](#)]
35. Peng, L.; Su, L.; Yu, X.; Wang, R.; Cui, X.; Tian, H.; Cao, S.; Xia, B.Y.; Shi, J. Electron Redistribution of Ruthenium-Tungsten Oxides Mott-Schottky Heterojunction for Enhanced Hydrogen Evolution. *Appl. Catal. B Environ.* **2022**, *308*, 121229. [[CrossRef](#)]
36. Li, N.; Zhang, L.; Wang, Y.; Zhou, S.; Zhang, Y.; Abd McKay, A.; Jin, Z.; Zhang, H.; Hu, G. Effect of In-Plane Mott-Schottky on the Hydroxyl Deprotonation in MoS<sub>2</sub>@Co<sub>3</sub>S<sub>4</sub>/NC Heterostructure for Efficient Overall Water Splitting. *J. Colloid Interface Sci.* **2023**, *649*, 125–131. [[CrossRef](#)] [[PubMed](#)]
37. Li, G.; Jang, H.; Liu, S.; Li, Z.; Kim, M.G.; Qin, Q.; Liu, X.; Cho, J. The Synergistic Effect of Hf-O-Ru Bonds and Oxygen Vacancies in Ru/HfO<sub>2</sub> for Enhanced Hydrogen Evolution. *Nat. Commun.* **2022**, *13*, 1270. [[CrossRef](#)]
38. Li, L.; Qiu, H.; Zhu, Y.; Chen, G.; She, S.; Guo, X.; Li, H.; Liu, T.; Lin, Z.; Zhou, H.; et al. Atomic Ruthenium Modification of Nickel-Cobalt Alloy for Enhanced Alkaline Hydrogen Evolution. *Appl. Catal. B Environ.* **2023**, *331*, 122710. [[CrossRef](#)]
39. Tiwari, J.N.; Harzandi, A.M.; Ha, M.; Sultan, S.; Myung, C.W.; Park, H.J.; Kim, D.Y.; Thangavel, P.; Singh, A.N.; Sharma, P.; et al. Hydrogen Evolution: High-Performance Hydrogen Evolution by Ru Single Atoms and Nitrided-Ru Nanoparticles Implanted on N-Doped Graphitic Sheet. *Adv. Energy Mater.* **2019**, *9*, 1970101. [[CrossRef](#)]
40. Ding, Y.; Cao, K.-W.; He, J.-W.; Li, F.-M.; Huang, H.; Chen, P.; Chen, Y. Nitrogen-Doped Graphene Aerogel-Supported Ruthenium Nanocrystals for pH-Universal Hydrogen Evolution Reaction. *Chin. J. Catal.* **2022**, *43*, 1535–1543. [[CrossRef](#)]
41. Wang, W.; Tang, H.; Liu, H.; Li, S.; Liu, G.; Zhang, W.; Wang, Y.; Wang, Q.; Liu, Q. Modified Graphene Supported Ruthenium as an Efficient Electrocatalyst for Hydrogen Evolution Reaction in Alkaline Media. *Catal. Lett.* **2023**. [[CrossRef](#)]

42. Yu, R.; Cao, X.; Chen, Q.; Li, W.; Huang, A.; Wei, X.; Mao, J. D-Band Center Optimization of Edge-Rich Ultrathin RuZn Nanosheets with Moiré Superlattices for pH-Universal Hydrogen Evolution Reaction. *Small* **2023**, *19*, e2303440. [[CrossRef](#)]
43. Zhang, J.; Chen, G.; Liu, Q.; Fan, C.; Sun, D.; Tang, Y.; Sun, H.; Feng, X. Competitive Adsorption: Reducing the Poisoning Effect of Adsorbed Hydroxyl on Ru Single-Atom Site with SnO<sub>2</sub> for Efficient Hydrogen Evolution. *Angew. Chem. Int. Ed.* **2022**, *134*, e202209486. [[CrossRef](#)]
44. Huang, X.; Lu, R.; Cen, Y.; Wang, D.; Jin, S.; Chen, W.; Geoffrey, L.; Waterhouse, N.; Wang, Z.; Tian, S.; et al. Micropore-Confined Ru Nanoclusters Catalyst for Efficient pH-Universal Hydrogen Evolution Reaction. *Nano Res.* **2023**, *16*, 9073–9080. [[CrossRef](#)]
45. Qin, X.; Ola, O.; Zhao, J.; Yang, Z.; Tiwari, S.K.; Wang, N.; Zhu, Y. Recent Progress in Graphene-Based Electrocatalysts for Hydrogen Evolution Reaction. *Nanomaterials* **2022**, *12*, 1806. [[CrossRef](#)]
46. Wu, C.; Ding, S.; Liu, D.; Li, D.; Chen, S.; Wang, H.; Qi, Z.; Ge, B.; Song, L. A Unique Ru-N<sub>4</sub>-P Coordinated Structure Synergistically Waking Up the Nonmetal P Active Site for Hydrogen Production. *Research* **2020**, *2020*, 5860712. [[CrossRef](#)]
47. Cao, L.; Luo, Q.; Chen, J.; Wang, L.; Lin, Y.; Wang, H.; Liu, X.; Shen, X.; Zhang, W.; Liu, W.; et al. Dynamic Oxygen Adsorption on Single-Atomic Ruthenium Catalyst with High Performance for Acidic Oxygen Evolution Reaction. *Nat. Commun.* **2019**, *10*, 4849. [[CrossRef](#)] [[PubMed](#)]
48. Xiao, M.; Gao, L.; Wang, Y.; Wang, X.; Zhu, J.; Jin, Z.; Liu, C.; Chen, H.; Li, G.; Ge, J.; et al. Engineering Energy Level of Metal Center: Ru Single-Atom Site for Efficient and Durable Oxygen Reduction Catalysis. *J. Am. Chem. Soc.* **2019**, *141*, 19800–19806. [[CrossRef](#)] [[PubMed](#)]
49. He, Q.; Zhou, Y.; Shou, H.; Wang, X.; Zhang, P.; Xu, W.; Qiao, S.; Wu, C.; Liu, H.; Liu, D.; et al. Synergic Reaction Kinetics over Adjacent Ruthenium Sites for Superb Hydrogen Generation in Alkaline Media. *Adv. Mater.* **2022**, *34*, 2110604. [[CrossRef](#)] [[PubMed](#)]
50. Zhang, R.; Du, X.; Li, S.; Guan, J.; Fang, Y.; Li, X.; Dai, Y.; Zhang, M. Application of Heteroatom Doping Strategy in Electrolyzed Water Catalytic Materials. *J. Electroanal. Chem.* **2022**, *921*, 116679. [[CrossRef](#)]
51. Wang, K.; Zhou, J.; Sun, M.; Lin, F.; Huang, B.; Lv, F.; Zeng, L.; Zhang, Q.; Gu, L.; Luo, M.; et al. Cu-Doped Heterointerfaced Ru/RuSe<sub>2</sub> Nanosheets with Optimized H and H<sub>2</sub>O Adsorption Boost Hydrogen Evolution Catalysis. *Adv. Mater.* **2023**, *35*, 2300980. [[CrossRef](#)]
52. Li, L.; Bu, L.; Huang, B.; Wang, P.; Shen, C.; Bai, S.; Chan, T.-S.; Shao, Q.; Hu, Z.; Huang, X. Compensating Electronic Effect Enables Fast Site-to-Site Electron Transfer over Ultrathin RuMn Nanosheet Branches toward Highly Electroactive and Stable Water Splitting. *Adv. Mater.* **2021**, *33*, 2105308. [[CrossRef](#)]
53. Liu, Q.; Zhang, C.; Wang, P.; Chen, D.; Xiao, M.; Chen, L.; Liu, S.; Yu, J.; Mu, S. Nearly Hollow Ru–Cu–MoO<sub>2</sub> Octahedrons Consisting of Clusters and Nanocrystals for High Efficiency Hydrogen Evolution Reaction. *J. Mater. Chem. A* **2022**, *10*, 12341–12349. [[CrossRef](#)]
54. Wu, X.; Wang, Z.; Zhang, D.; Qin, Y.; Wang, M.; Han, Y.; Zhan, T.; Yang, B.; Li, S.; Lai, J.; et al. Solvent-Free Microwave Synthesis of Ultra-Small Ru-Mo<sub>2</sub>C@CNT with Strong Metal-Support Interaction for Industrial Hydrogen Evolution. *Nat. Commun.* **2021**, *12*, 4018. [[CrossRef](#)]
55. Liu, J.; Ding, G.; Yu, J.; Liu, X.; Zhang, X.; Guo, J.; Zhang, J.; Ren, W.; Che, R. Visualizing Spatial Potential and Charge Distribution in Ru/N-Doped Carbon Electrocatalysts for Superior Hydrogen Evolution Reaction. *J. Mater. Chem. A* **2019**, *7*, 18072–18080. [[CrossRef](#)]
56. Yu, J.; Wang, A.; Yu, W.; Liu, X.; Li, X.; Liu, H.; Hu, Y.; Wu, Y.; Zhou, W. Tailoring the Ruthenium Reactive Sites on N Doped Molybdenum Carbide Nanosheets via the Anti-Ostwald Ripening as Efficient Electrocatalyst for Hydrogen Evolution Reaction in Alkaline Media. *Appl. Catal. B Environ.* **2020**, *277*, 119236. [[CrossRef](#)]
57. Chen, J.; Chen, C.; Qin, M.; Li, B.; Lin, B.; Mao, Q.; Yang, H.; Liu, B.; Wang, Y. Reversible Hydrogen Spillover in Ru-WO<sub>3-x</sub> Enhances Hydrogen Evolution Activity in Neutral pH Water Splitting. *Nat. Commun.* **2022**, *13*, 5382. [[CrossRef](#)]
58. Zeng, Y.; Zhao, M.; Huang, Z.; Zhu, W.; Zheng, J.; Jiang, Q.; Wang, Z.; Liang, H. Surface Reconstruction of Water Splitting Electrocatalysts. *Adv. Energy Mater.* **2022**, *12*, 2201713. [[CrossRef](#)]
59. Lao, M.; Li, P.; Jiang, Y.; Pan, H.; Dou, S.X.; Sun, W. From fundamentals and theories to heterostructured electrocatalyst design: An in-depth understanding of alkaline hydrogen evolution reaction. *Nano Energy* **2022**, *98*, 107231. [[CrossRef](#)]
60. Chen, X.; Wang, X.-T.; Le, J.-B.; Li, S.-M.; Wang, X.; Zhang, Y.-J.; Radjenovic, P.; Zhao, Y.; Wang, Y.-H.; Lin, X.-M.; et al. Revealing the Role of Interfacial Water and Key Intermediates at Ruthenium Surfaces in the Alkaline Hydrogen Evolution Reaction. *Nat. Commun.* **2023**, *14*, 5289. [[CrossRef](#)] [[PubMed](#)]
61. Sun, K.; Wu, X.; Zhuang, Z.; Liu, L.; Fang, J.; Zeng, L.; Ma, J.; Liu, S.; Li, J.; Dai, R.; et al. Interfacial Water Engineering Boosts Neutral Water Reduction. *Nat. Commun.* **2022**, *13*, 6260. [[CrossRef](#)] [[PubMed](#)]
62. Liu, X.; He, L.; Han, G.; Sheng, J.; Yu, Y.; Yang, W. Design of Rich Defects Carbon Coated MnFe<sub>2</sub>O<sub>4</sub>/LaMnO<sub>3</sub>/LaFeO<sub>3</sub> Heterostructure Nanocomposites for Broadband Electromagnetic Wave Absorption. *Chem. Eng. J.* **2023**, *476*, 146199. [[CrossRef](#)]
63. Wang, Y.; Bao, S.; Liu, X.; Qiu, L.; Sheng, J.; Yang, W.; Yu, Y. Regulating the Peroxymonosulfate Activation on N Doped δ-MnO<sub>2</sub> Nanosheets for Tetracycline Degradation: N Species as the Degradation Pathways Switcher to Convert Radical to Nonradical. *Chem. Eng. J.* **2023**, *477*, 147050. [[CrossRef](#)]
64. Wang, Y.; Qiu, L.; Bao, S.; Tian, F.; Sheng, J.; Yang, W.; Yu, Y. Visible-Light Enhanced Peroxymonosulfate Activation on Co<sub>3</sub>O<sub>4</sub>/MnO<sub>2</sub> for the Degradation of Tetracycline: Cooperation of Radical and Non-Radical Mechanisms. *Sep. Purif. Technol.* **2023**, *316*, 123779. [[CrossRef](#)]

65. Mohammed-Ibrahim, J.; Sun, X. Recent Progress on Earth Abundant Electrocatalysts for Hydrogen Evolution Reaction (HER) in Alkaline Medium to Achieve Efficient Water Splitting—A Review. *J. Energy Chem.* **2019**, *34*, 111–160. [[CrossRef](#)]
66. Lin, F.; Li, M.; Zeng, L.; Luo, M.; Guo, S. Intermetallic Nanocrystals for Fuel-Cells-Based Electrocatalysis. *Chem. Rev.* **2023**, *123*, 12507–12593. [[CrossRef](#)]
67. Jiang, Y.; Yang, K.; Li, M.; Xu, D.; Ma, Z. Engineering the Spin Configuration of Electrocatalysts for Electrochemical Renewable Conversions. *Mater. Chem. Front.* **2024**. [[CrossRef](#)]

**Disclaimer/Publisher’s Note:** The statements, opinions and data contained in all publications are solely those of the individual author(s) and contributor(s) and not of MDPI and/or the editor(s). MDPI and/or the editor(s) disclaim responsibility for any injury to people or property resulting from any ideas, methods, instructions or products referred to in the content.